J Appl Physiol 120: 1132–1140, 2016.
First published March 17, 2016; doi:10.1152/japplphysiol.00007.2016.

Intestinal and sublingual microcirculation are more severely compromised in hemodilution than in hemorrhage

Gonzalo Ferrara,[1] Vanina Siham Kanoore Edul,[1] Enrique Martins,[1] Héctor Saúl Canales,[1] Carlos Canullán,[1] Gastón Murias,[1] Mario Omar Pozo,[1] Elisa Estenssoro,[1] Can Ince,[2] and Arnaldo Dubin[1]

[1]*Cátedra de Farmacología Aplicada, Facultad de Ciencias Médicas, Universidad Nacional de La Plata, La Plata, Argentina; and* [2]*Academic Medical Center, Department of Translational Physiology, University of Amsterdam, Amsterdam, The Netherlands*

Submitted 4 January 2016; accepted in final form 10 March 2016

Ferrara G, Kanoore Edul VS, Martins E, Canales HS, Canullán C, Murias G, Pozo MO, Estenssoro E, Ince C, Dubin A. Intestinal and sublingual microcirculation are more severely compromised in hemodilution than in hemorrhage. *J Appl Physiol* 120: 1132–1140, 2016. First published March 17, 2016; doi:10.1152/japplphysiol.00007.2016.—The alterations in O_2 extraction in hemodilution have been linked to fast red blood cell (RBC) velocity, which might affect the complete release of O_2 from Hb. Fast RBC velocity might also explain the normal mucosal-arterial P_{CO_2} (ΔP_{CO_2}). Yet sublingual and intestinal microcirculation have not been completely characterized in extreme hemodilution. Our hypothesis was that the unchanged ΔP_{CO_2} in hemodilution depends on the preservation of villi microcirculation. For this purpose, pentobarbital-anesthetized and mechanically ventilated sheep were submitted to stepwise hemodilution ($n = 8$), hemorrhage ($n = 8$), or no intervention (sham, $n = 8$). In both hypoxic groups, equivalent reductions in O_2 consumption ($\dot{V}_{O_2}$) were targeted. Microcirculation was assessed by videomicroscopy, intestinal ΔP_{CO_2} by air tonometry, and $\dot{V}_{O_2}$ by expired gases analysis. Although cardiac output and superior mesenteric flow increased in hemodilution, from the very first step (Hb = 5.0 g/dl), villi functional vascular density and RBC velocity decreased (21.7 ± 0.9 vs. 15.9 ± 1.0 mm/mm^2 and 1,033 ± 75 vs. 850 ± 79 μm/s, $P < 0.01$). In the last stage (Hb = 1.2 g/dl), these variables were lower in hemodiution than in hemorrhage (11.1 ± 0.5 vs. 15.4 ± 0.9 mm/mm^2 and 544 ± 26 vs. 686 ± 70 μm/s, $P < 0.01$), and were associated with lower intestinal fractional O_2 extraction (0.61 ± 0.04 vs. 0.79 ± 0.02, $P < 0.01$) but preserved ΔP_{CO_2} (5 ± 2 vs. 25 ± 4 mmHg, $P < 0.01$). Therefore, alterations in O_2 extraction in hemodilution seemed related to microvascular shunting, not to fast RBC velocity. The severe microvascular abnormalities suggest that normal ΔP_{CO_2} was not dependent on CO_2 washout by the villi microcirculation. Increased perfusion in deeper intestinal layers might be an alternative explanation.

microcirculation; P_{CO_2}; hypoxia; anemia; hemorrhage

NEW & NOTEWORTHY

This study showed that in the systemic hyperdynamic state of hemodilution, intestinal and sublingual microcirculation were more severely compromised than in hemorrhage. Consequently, the decreased ability to increase O_2 extraction could result from microcirculatory shunting, and not from failure in O_2 dissociation from Hb. Despite the severe villi hypoperfusion, tissue P_{CO_2} was normal, which could be ascribed to CO_2 clearance in the deeper intestinal layers.

Address for reprint requests and other correspondence: A. Dubin, Cátedra de Farmacología Aplicada, Facultad de Ciencias Médicas, Universidad Nacional de La Plata, Calle 42 N° 577 (1900), La Plata, Argentina (e-mail: arnaldodubin@gmail.com).

TISSUE HYPOXIA can result from three basic mechanisms: hypoxemia, ischemia, and isovolemic anemia. When O_2 delivery ($\dot{D}_{O_2}$) decreases beyond a critical point, O_2 utilization ($\dot{V}_{O_2}$) becomes supply dependent, regardless of the cause of hypoxia (34). This limitation in $\dot{V}_{O_2}$ can depend on diffusional factors such as the gradient between capillary and mitochondrial P_{O_2}, or on the rate of the convective O_2 transport to the capillaries. Although similar values of critical $\dot{D}_{O_2}$ have been found in hypoxic and anemic hypoxia, venous P_{O_2} was found to be higher in anemic hypoxia (9). This suggests that the limitation in tissue oxygenation results from the reduction in convective $\dot{D}_{O_2}$ rather than from the decreased driving pressure for O_2 diffusion. It has been shown, however, that the different venous P_{O_2} found in hypoxic and anemic hypoxia correspond to the same tissue P_{O_2} (24). Therefore, diffusional mechanisms might also play a major role in limiting aerobic metabolism.

Fast microcirculatory velocity associated with hemodilution might explain the higher venous P_{O_2} found in anemic hypoxia, since shorter erythrocyte transit time could affect the complete release of O_2 from the Hb (25). Nevertheless, a parallel decrease in intestinal microvascular O_2 saturation and P_{O_2} has been described, suggesting that the venous-capillary P_{O_2} gap was not primarily caused by an O_2 unload deficit (35). Another likely explanation for the P_{O_2} gap might be the presence of microvascular shunting.

The characteristics of microcirculation during extreme hemodilution have not been completely described, especially in the gut. For example, in the hamster striated skin muscle, capillary density decreased during anemic hypoxia, whereas red blood cell (RBC) velocity increased and decreased afterward when higher levels of hemodilution were achieved (7). In contrast, hemodilution induced progressive increases in cerebral RBC velocity (27). Accordingly, the gut mucosal P_{CO_2}—an indicator of microvascular perfusion—remained remarkably stable during the O_2 supply dependency induced by extreme hemodilution (15). These results may be interpreted as evidence of preserved villi microcirculation.

To further clarify the behavior of villi microcirculation in anemic hypoxia and its relationship with mucosal P_{CO_2}, we carried out a study in sheep submitted to a stepwise hemodilution. We compared these sheep with another group, in which we performed a progressive bleeding to reach equivalent reductions in $\dot{V}_{O_2}$. Our hypothesis was that the lack of change in tissue P_{CO_2} in anemic hypoxia depends on the preservation of mucosal microvascular blood flow.

MATERIALS AND METHODS

Anesthesia and ventilation. This study was approved by the local Animal Research Committee (0800-009634/11-000). Care of animals was in accordance with National Institutes of Health (United States). Twenty-four sheep (21 ± 7 kg, means ± SD) were anesthetized with 30 mg/kg of pentobarbital sodium, intubated, and mechanically ventilated with a Servo Ventilator 900C (Siemens-Elema, Solna, Sweden) with a tidal volume of 15 ml/kg, an inspired O_2 fraction of 0.21, and a positive end-expiratory pressure of 6 cm H_2O. The initial respiratory rate was set to keep the arterial P_{CO_2} between 35 and 40 mmHg. This respiratory setting was maintained during the rest of the experiment. Neuromuscular blockade was performed with pancuronium bromide (0.06 mg/kg). Additional pentobarbital boluses (1 mg/kg) were administered hourly and when clinical signs of inadequate depth of anesthesia were evident. Analgesia was provided by fentanyl as a bolus of 2 μg/kg, followed by 1 $\mu g \cdot h^{-1} \cdot kg^{-1}$. These drugs were administered intravenously.

Surgical preparation. A 7.5 French Swan-Ganz Standard Thermodilution Pulmonary Artery Catheter (Edwards Life Sciences, Irvine, CA) was inserted through an introducer in the right external jugular vein to obtain mixed venous samples; its side port was used to administer fluids and drugs. Catheters were placed in the descending aorta via the left femoral artery to measure blood pressure, perform the bleeding, and obtain blood samples. Catheters were also placed and in the inferior vena cava to infuse fluids during isovolemic hemodilution.

A midline laparotomy was performed, followed by a gastrostomy to drain gastric contents, and a splenectomy to avoid spleen contraction during the hemorrhage. An electromagnetic flow probe was placed around superior mesenteric artery to measure intestinal blood flow. A catheter was introduced in the mesenteric vein through a small vein proximal to the gut to draw blood samples and to measure pressure. A tonometer was inserted through a small ileotomy to measure intramucosal P_{CO_2}. A 10- to 15-cm segment of the ileum was mobilized, placed outside the abdomen, and opened 2 cm on the antimesenteric border to allow an examination of mucosal microcirculation. The exteriorized intestinal segment was covered and moisture and temperature preserved by a device. Finally, after complete hemostasis, the abdominal wall incision was closed, excepting a short segment for externalization of the ileal loop.

Measurements and derived calculations. Systemic $\dot{V}_{O_2}$, CO_2 production ($\dot{V}_{CO_2}$), and respiratory exchange ratio (RER) were measured by analysis of expired gases (MedGraphics CPX Ultima, Medical Graphics, St. Paul, MN). $\dot{V}_{O_2}$ and $\dot{V}_{CO_2}$ were adjusted to body weight.

Arterial, mixed venous and mesenteric venous P_{O_2}, P_{CO_2}, pH, Hb, and O_2 saturation were measured with a blood gas analyzer and a CO-oximeter (ABL 5 and OSM 3, Radiometer, Copenhagen, Denmark). The respective O_2 contents were calculated by standard formulae. Systemic and intestinal fractional O_2 extraction were calculated as arterial minus mixed venous O_2 content divided arterial O_2 content and arterial minus mesenteric venous O_2 content divided arterial O_2 content, respectively. We also calculated the mixed venous minus arterial and the mesenteric venous minus arterial P_{CO_2} differences.

Cardiac output was calculated as $\dot{V}_{O_2}$ divided by arterial minus mixed venous O_2 content difference. Systemic $\dot{D}_{O_2}$ was calculated as cardiac output by arterial O_2 content.

Intestinal blood flow was measured by the electromagnetic method (Spectramed Blood Flowmeter model SP 2202 B, Spectramed, Oxnard, CA), with in vitro calibrated transducers of 5-7 mm of diameter (Blood Flowmeter Transducer, Spectramed). Occlusive zero was controlled before and after each experiment. Nonocclusive zero was corrected before each measurement. Superior mesenteric blood flow (SMABF) was referred to gut weight. Intestinal $\dot{D}_{O_2}$ was calculated as SMABF by arterial O_2 content and intestinal $\dot{V}_{O_2}$ as SMABF by arterial minus mesenteric venous O_2 content difference.

Intramucosal P_{CO_2} was measured with a tonometer (Tonometrics Catheter, Datex-Ohmeda, Helsinki, Finland) through the use of an automated air tonometry system (Tonocap, Datex-Ohmeda, Helsinki, Finland). Its value was used to calculate intramucosal-arterial P_{CO_2} (ΔP_{CO_2}).

Arterial lactate was measured with a point-of-care analyzer (Stat Profile Critical Care Xpress, Nova Biomedical, Waltham, MA).

Microvideoscopic measurements and analysis. The microcirculatory network was evaluated in the intestinal mucosa and serosa, and the sublingual mucosa by means of a sidestream dark field (SDF) imaging device (Microscan, MicroVision Medical, Amsterdam, The Netherlands) (23). Different precautions were taken and steps followed to obtain images of adequate quality and to insure satisfactory reproducibility. After gentle removal of saliva by isotonic saline–drenched gauze, steady images of at least 20 s were obtained while avoiding pressure artifacts with a portable computer and an analog-to-digital video converter (ADVC110, Canopus, San Jose, CA). The videos were recorded from five different areas. Video clips were stored as AVI files to allow computerized frame-by-frame image analysis. Typical normal and pathological images are available as Supplemental Material (Supplemental Material for this article is available online at the Journal website).

Video image analysis was performed blindly by well-trained researchers. Adequate focus and contrast adjustment were verified, and images of poor quality were discarded. The entire sequence was used to describe the semiquantitative characteristics of the microvascular flow and, particularly, the presence of stopped or intermittent flow.

We used an image analysis software developed for the SDF video images (Microscan analysis software AVA 3.0 MicroVision Medical, Amsterdam, The Netherlands) (13) to determine the total vascular density. An analysis based on semiquantitative criteria that distinguished between no flow (0 au), intermittent flow (1 au), sluggish flow (2 au), and continuous flow (3 au) was performed on individual vessels (3). The overall score, called the microvascular flow index, is the average of the individual values (32). Quantitative RBC velocity was determined through the use of space-time diagrams (13). We also calculated the proportion of perfused vessels and the functional vascular density (i.e., the total vascular density multiplied by the fraction of perfused vessels). The flow heterogeneity was evaluated as the coefficient of variation of RBC velocity.

In sheep, most of sublingual vascular density (97 ± 1%) and all intestinal vessels consist of small vessels (diameter below 25 μm) (18), so the analysis was focused on these types of vessels, whereas the vessels of higher diameter were assessed only for ruling out compression artifacts.

Experimental procedure. Basal measurements were taken after a period of no less than 30 min after systemic $\dot{V}_{O_2}$ and $\dot{V}_{CO_2}$, and intestinal blood flow became stable. Animals were then assigned to hemodilution ($n = 8$), hemorrhage ($n = 8$), or sham ($n = 8$) groups. In the hemodilution group, we performed a stepwise hemodilution through isovolemic exchange of blood with 6% hydroxyethylstarch 130/0.4 in 0.9% NaCl (Voluven, Fresenius Kabi, Bad Homburg, Germany). The amount of blood exchanged to reach desired levels of hematocrit of about 0.15, 0.10, and 0.05 in each step was estimated as previously referred (4). In the hemorrhage group, consecutive bleedings of 5–10 ml/kg were performed. Similar reductions in systemic and intestinal $\dot{V}_{O_2}$ were pursued in in both hypoxic groups. In the sham group, the same experimental preparation was carried out, and 0.9% NaCl was infused to maintain hemodynamic variables at basal values, without further interventions. Measurements were performed at 30, 60, and 90 min, except for microcirculatory videos, which were only acquired at baseline and in the first and the last stage of hemodilution or bleeding (0, 30, and 90 min). Blood temperature was kept constant throughout the study with a heating lamp.

At the end of the experiment, the animals were killed with an additional dose of pentobarbital and a KCl bolus. A catheter was inserted in the superior mesenteric artery and Indian ink was instilled

through it. Dyed intestinal segments were dissected, washed, and weighed to calculate gut indexes.

Data analysis. Using the functional vascular density of the intestinal mucosa as the primary measure of outcome and taking into consideration values previously found in control sheep (15), we calculated that eight sheep were needed in each group to detect a difference of 25%, with a power of 80% and a certainty of 95%.

Data were assessed for normality and expressed as means ± SE. Groups were compared with two-way repeated measures of ANOVA. After a $P < 0.05$ for time × group interaction, a post hoc Student *t*-test with Bonferroni correction was used for pairwise comparisons.

RESULTS

Effects on systemic and regional hemodynamics. In the hemodilution group, mean arterial pressure decreased in the last stage, while cardiac index and SMABF increased from the first stage. In the hemorrhage group, there were progressive decreases in blood pressure, cardiac index, and SMABF. The fraction of cardiac output directed to the superior mesenteric artery remained unchanged in the three groups. Pulmonary occlusion and mesenteric venous pressures increased in hemodilution (Table 1).

Effects on $\dot{D}o_2$ and $\dot{V}o_2$. In both types of hypoxia, there were significant reductions in systemic and intestinal $\dot{D}o_2$ and $\dot{V}o_2$ (Fig. 1). Oxygen supply dependency was produced by reductions in Hb levels in hemodilution, and in blood flow in hemorrhage, respectively. In hemorrhage, there were also decreases in Hb but values were significantly higher than in hemodilution (Table 1). There were concomitant increases in

Table 1. *Values of hemoglobin and systemic and intestinal hemodynamic variables in sham, ischemic hypoxia, and anemic hypoxia groups*

	Basal	30 Min	60 Min	90 Min
Body weight, kg				
Sham	25 ± 3			
Hemorrhage	22 ± 2			
Hemodilution	19 ± 1			
Age, mo				
Sham	165 ± 14			
Hemorrhage	144 ± 15			
Hemodilution	123 ± 11			
Hemoglobin, g/dl				
Sham	10.0 ± 0.6	10.0 ± 0.6	9.9 ± 0.6	9.9 ± 0.6
Hemorrhage	8.4 ± 0.5	7.9 ± 0.4*†	7.6 ± 0.5*†	6.6 ± 0.4*†
Hemodilution	8.3 ± 0.4	5.0 ± 0.4*†‡	3.2 ± 0.2*†‡	1.2 ± 0.1*†‡
Heart rate, beats/min				
Sham	167 ± 6	170 ± 2	171 ± 2	161 ± 11
Hemorrhage	140 ± 13	117 ± 16	124 ± 17	149 ± 17
Hemodilution	143 ± 8	167 ± 13	166 ± 11	170 ± 12
Mean arterial pressure, mmHg				
Sham	93 ± 4	97 ± 4	96 ± 3	99 ± 4
Hemorrhage	85 ± 5	43 ± 5*†	39 ± 3*†	27 ± 2*†
Hemodilution	83 ± 3	86 ± 4‡	88 ± 5‡	59 ± 4*†‡
Central venous pressure, mmHg				
Sham	2 ± 1	2 ± 1	2 ± 1	2 ± 1
Hemorrhage	3 ± 1	3 ± 1	4 ± 1	3 ± 1
Hemodilution	3 ± 1	4 ± 1	4 ± 1	6 ± 2
Mean pulmonary pressure, mmHg				
Sham	12 ± 1	13 ± 1	14 ± 1	13 ± 1
Hemorrhage	16 ± 2	12 ± 2*	11 ± 2*	10 ± 1*
Hemodilution	16 ± 2	21 ± 3‡	21 ± 2†‡	18 ± 2‡
Pulmonary occlusion pressure, mmHg				
Sham	3 ± 1	3 ± 1	3 ± 1	3 ± 1
Hemorrhage	5 ± 1	5 ± 1	5 ± 1	5 ± 2
Hemodilution	4 ± 1	6 ± 1*†	7 ± 1*†	8 ± 2*†
Mesenteric venous pressure, mmHg				
Sham	5 ± 1	6 ± 1	6 ± 1	5 ± 1
Hemorrhage	5 ± 1	4 ± 1	5 ± 1	4 ± 1
Hemodilution	5 ± 1	6 ± 1*‡	7 ± 1*‡	8 ± 1*‡
Cardiac index, $ml \cdot min^{-1} \cdot kg^{-1}$				
Sham	112 ± 10	114 ± 9	112 ± 13	125 ± 19
Hemorrhage	166 ± 13	126 ± 32	92 ± 13*	54 ± 6*†
Hemodilution	165 ± 16	230 ± 16*†‡	300 ± 34*†‡	373 ± 41†‡
Superior mesenteric artery flow, $ml \cdot min^{-1} \cdot 100\ g^{-1}$				
Sham	58 ± 6	63 ± 9	56 ± 6	56 ± 7
Hemorrhage	80 ± 90	46 ± 7*	43 ± 5*	23 ± 4*†
Hemodilution	82 ± 13	97 ± 14*‡	116 ± 24*†‡	122 ± 11*†‡
Superior mesenteric flow/cardiac output, %				
Sham	16 ± 2	16 ± 1	16 ± 1	14 ± 1
Hemorrhage	22 ± 4	18 ± 3	20 ± 2	14 ± 2
Hemodilution	18 ± 2	16 ± 2	16 ± 2	18 ± 2

Data are shown as means ± SE. *$P < 0.05$ vs. basal; †$P < 0.05$ vs. sham; ‡$P < 0.05$ vs. hemorrhage.

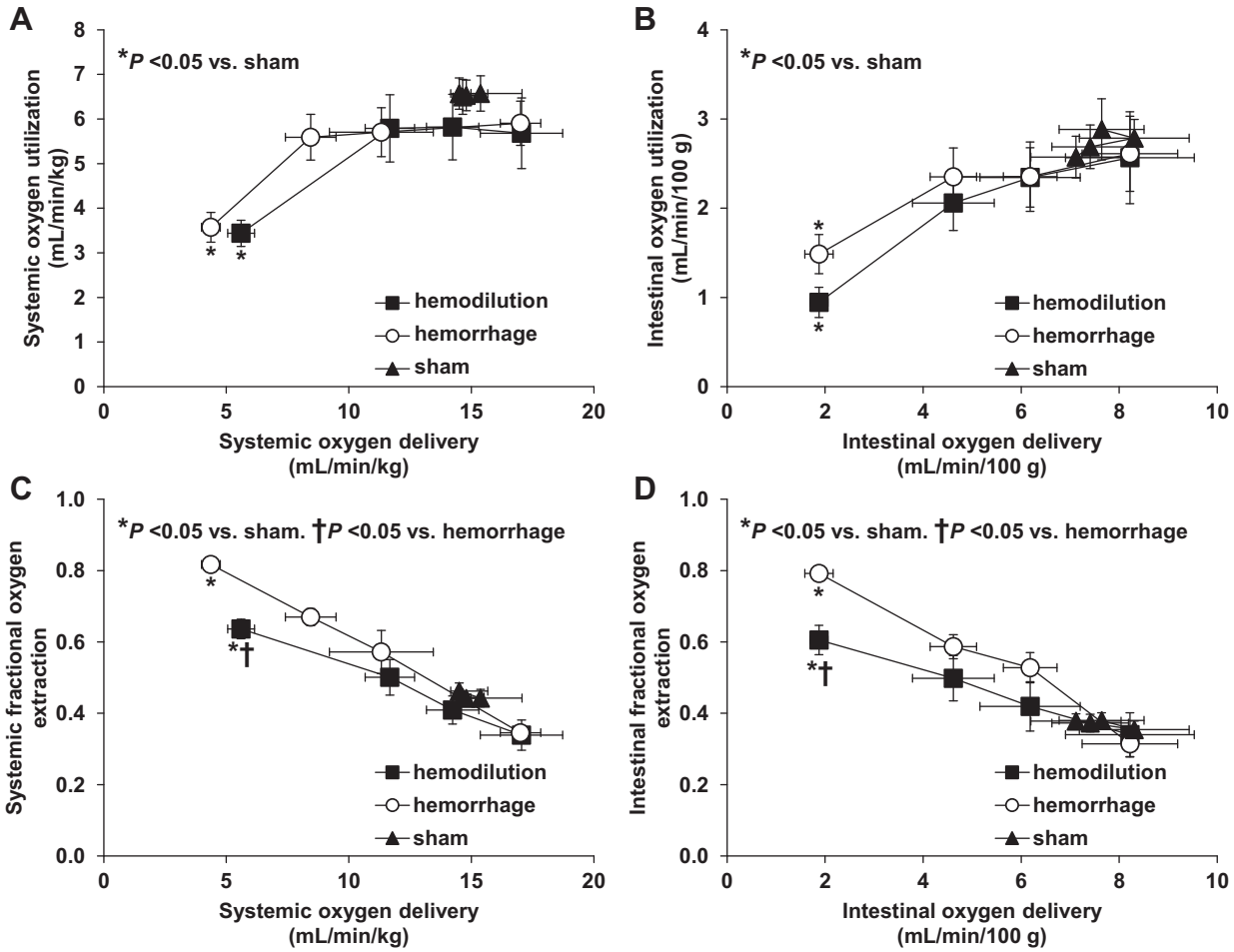

Fig. 1. Systemic and intestinal O_2 delivery and utilization in sham, hemorrhage, and hemodilution groups. *A*: relationship between systemic O_2 delivery and utilization. *B*: relationship between intestinal O_2 delivery and utilization. *C*: relationship between systemic O_2 delivery and fractional O_2 extraction. *D*: relationship between intestinal O_2 delivery and intestinal fractional O_2 extraction. *$P < 0.05$ vs. sham and †$P < 0.05$ vs. hemorrhage for time × group interaction of systemic O_2 utilization (*A*), intestinal O_2 utilization (*B*), systemic fractional O_2 extraction (*C*), and intestinal fractional O_2 extraction. The reductions in systemic and intestinal O_2 utilization were similar in hemorrhage and hemodilution, but the increases in the fractional O_2 extraction were higher in hemorrhage. In the last stage, systemic O_2 delivery was lower in both hypoxic groups compared with sham, but the decrease was greater in hemorrhage compared with hemodilution ($P < 0.05$). These significances are not displayed in the figures.

systemic and intestinal fractional O_2 extraction, which were higher in hemorrhage than in hemodilution (Fig. 1). In the last stage, systemic and intestinal $\dot{V}O_2$ were similarly reduced in both hypoxic groups, but systemic $\dot{D}O_2$ was higher in hemodilution than in hemorrhage. Comparable increases in RER and lactate levels developed in both hypoxic groups (Fig. 2). Systemic and intestinal O_2-derived variables and lactate levels remained unchanged in the sham group (Figs. 1 and 2).

Effects on CO_2 metabolism. In the last stage the decrease in $\dot{V}CO_2$, compared with the sham group, only reached statistical significance in the hemorrhage group (4.7 ± 0.3, 3.6 ± 0.3, and 3.9 ± 0.4 ml·min^{-1}·kg^{-1}, $P < 0.05$). Systemic and intestinal venoarterial PCO_2 differences and ΔPCO_2 increased in hemorrhage and did not change in hemodilution and sham groups (Figs. 2 and 3 and Supplemental Material).

Effects on microcirculation. In the intestinal mucosa the total and functional vascular density, the proportion of perfused vessels, the microvascular flow index, and the RBC velocity decreased, and the coefficient of variation of RBC velocity increased in hemorrhage and hemodilution compared with sham group. The alterations in the total and functional vascular density and the RBC velocity were more severe in hemodilution than in hemorrhage group (Fig. 4). A similar pattern was observed in intestinal serosa and sublingual mucosa, except for the coefficient of variation of RBC velocity, which remained stable (Figs. 2 and 3 and Supplemental Material). Microcirculatory variables did not change in sham group. In the hemodilution group there were significant correlations between Hb and both RBC velocity and functional vascular density in the three microvascular beds (Fig. 5).

DISCUSSION

Several studies have characterized microcirculation during hemodilution. Nevertheless, this is the first study that compares, in different microvascular beds, the effects of extreme isovolemic hemodilution with those of hemorrhage. It also includes a comprehensive evaluation of systemic and intestinal O_2 and CO_2 metabolism. Our main findings were the following: *1*) the key diffusional and convective determinants of the microvascular O_2 transport—capillary density and RBC velocity—were more severely compromised in hemodilution than in

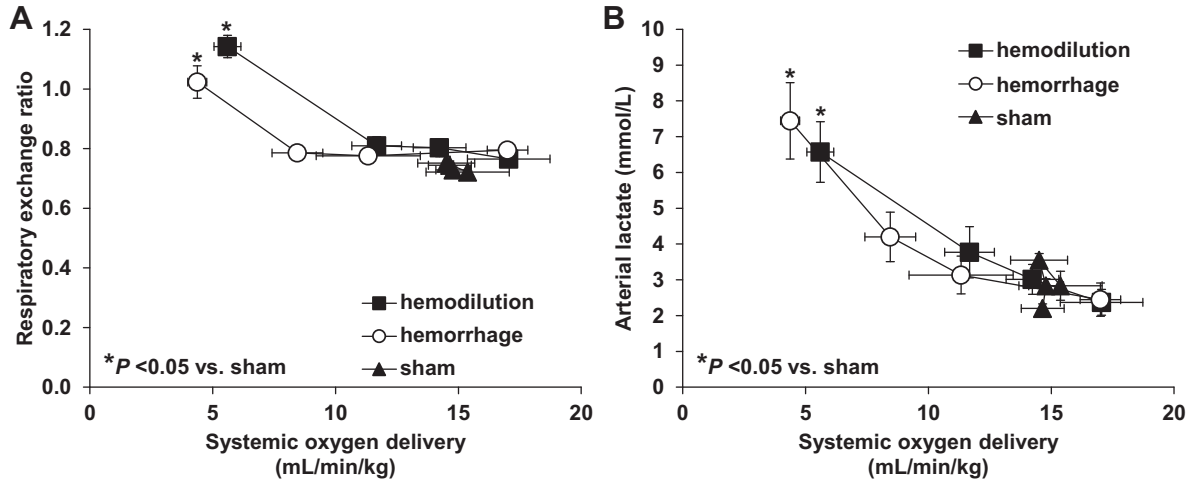

Fig. 2. Respiratory exchange ratio (*A*) and arterial lactate (*B*) in sham, hemorrhage, and hemodilution groups. Similar increases in both variables developed in the last stage of hemorrhage and hemodilution. There were no changes in the sham group.

hemorrhage; *2*) as a result of this, the defect in O_2 extraction found in the hyperdynamic condition of anemic hypoxia might not be related to reduced capillary transit time and decreased O_2 release from hemoglobin, but to microcirculatory shunting; and *3*) there was an absence of mucosal hypercarbia (normal ΔP_{CO_2}), which cannot be explained by the clearance of CO_2 through the villi perfusion, given the profound microvascular abnormalities.

Contrary to the intuitive consideration that the high systemic and regional blood flow of anemic hypoxia is uniformly associated with hyperdynamic tissue perfusion, previous studies have showed a contrasting behavior of the microcirculation among different territories. For example, in the rabbit tenuissimus muscle, isovolemic hemodilution to a hematocrit of 17 ± 2% increased RBC velocity by 45% (31). Similar results were reported in the hamster skinfold model when Hb levels decreased to ~6 g/dl. Further hemodilution to values of ~4 g/dl, however, reduced the RBC velocity compared with baseline. The changes in RBC velocity occurred with a progressive decrease in functional capillary density (5, 7). These alterations were even more severe when hemodilution reached extreme values, comparable with ours (Hb = 1.1 g/dl) (38). A similar pattern was described in the skin of the rat (33). In contrast to the U-shaped behavior of RBC velocity in muscle and skin, the relationship in the central nervous system (27, 28) and in the heart (2) was found to be linear.

Despite all this information about the microcirculation in hemodilution, our findings are original on some points. This is the first study on isovolemic hemodilution that assessed the microcirculation by direct and simultaneous visualization of intestinal mucosa and serosa, and sublingual mucosa. The experimental model consisted in progressive hemodilution, which, different to most studies, reached a critical $\dot{D}o_2$. Besides, we compared the effects of similar reductions in $\dot{V}o_2$ produced by extreme hemodilution and hemorrhage.

We showed a progressive alteration in the diffusional and convective determinants of tissue perfusion from the very first stage of hemodilution, when Hb was decreased to 5.0 g/dl. These variables were further impaired in the last stage, in which an Hb of 1.2 g/dl was reached. At this point, microvascular derangements were more pronounced in hemodilution than in hemorrhage, and increased flow heterogeneity appeared in the villi. In the hemodilution group the changes in RBC velocity and functional vascular density were strongly correlated with Hb levels. Our findings differ from those found in other vascular beds such as skin, striated muscle, heart, and brain (2, 5, 7, 27, 28, 31, 33). These differences could result from a different microvascular control in each territory but also from the method used in the assessment. In most of the mentioned studies, conventional videomicroscopy was used, whereas we used SDF technology. These techniques have not been directly compared with each other, but both are interchangeable with orthogonal polarizing spectroscopy (OPS) videomicroscopy (23, 26).

Since intestinal regional flow increased and the fraction of cardiac output directed to the gut remained unchanged, the intestinal microvascular alterations cannot be ascribed to flow redistribution to vital organs (35), but to the development of intramural shunting. This phenomenon affected intestinal mucosa and serosa to the same extent, as shown by equivalent

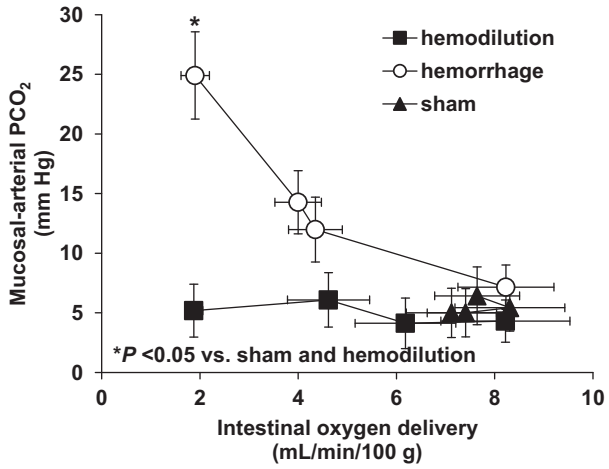

Fig. 3. Tissue mucosal-arterial P_{CO_2} difference as a function of intestinal O_2 delivery in sham, hemorrhage, and hemodilution groups. The gradients increased in the hemorrhage and remained unchanged in the hemodilution and sham groups.

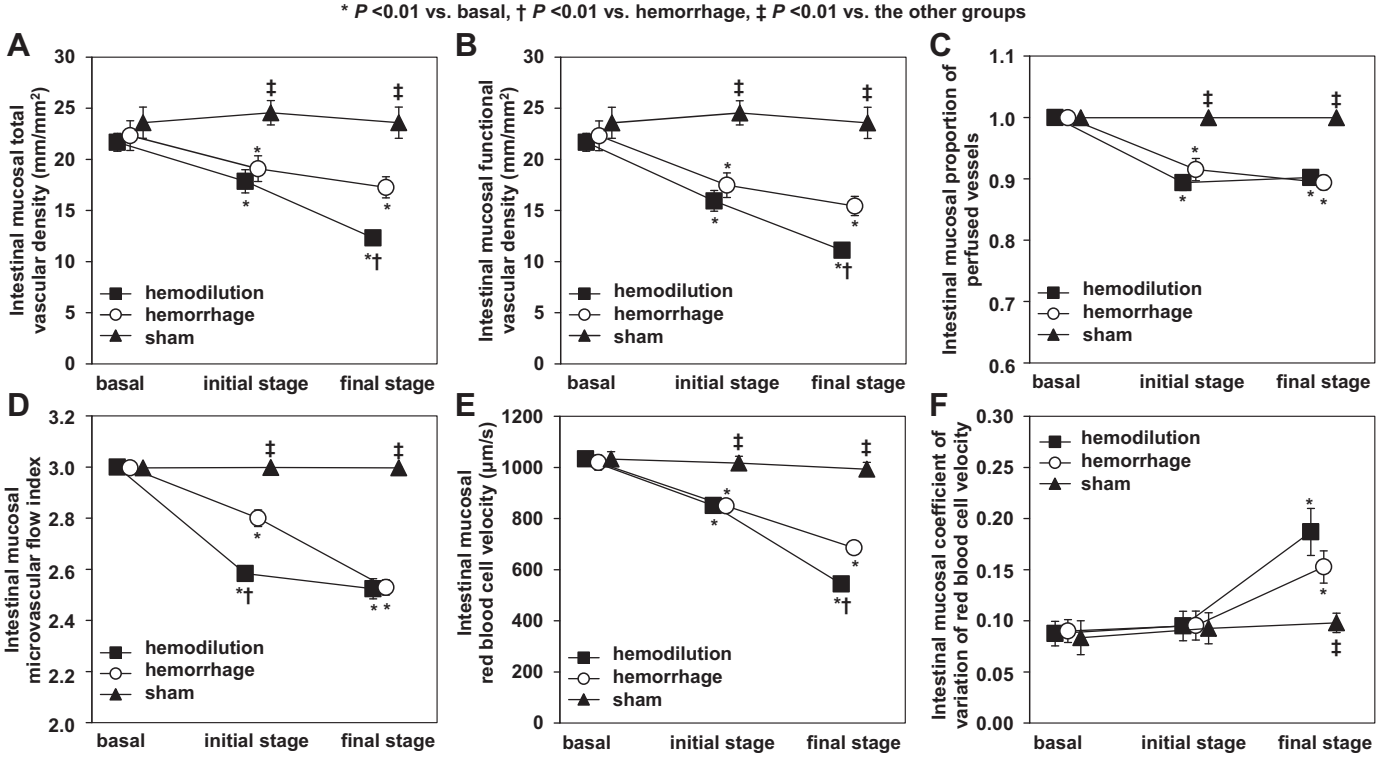

Fig. 4. Microcirculatory variables in the intestinal mucosa. *A*: total vascular density. *B*: functional vascular density. *C*: proportion of perfused vessels. *D*: microvascular flow index. *E*: red blood cell velocity. *F*: coefficient of variation of red blood cell velocity. Every microvascular variable was altered in hemorrhage and hemodilution compared with the sham group. In the last stage the alterations in total and functional vascular density and red blood cell velocity were more severe in hemodilution than in hemorrhage.

reductions in the microvascular variables. The difference was that only the villi, and not the serosa, exhibited an increased heterogeneity. Another study, however, reported that microvascular oxygenation was preserved in the mucosa, but not in the serosa (35). In this study, serosal and mucosal microvascular P_{O_2} were measured by the quenching of Pd-porphyrin phosphorescence. This method has a penetration depth of ~0.5 mm (36), almost comprising the total thickness of each layer. It might not notice the alterations in the most superficial villi microvessels, which are appropriately visualized by SDF videomicroscopy.

The heterogeneity described among different microvascular territories emphasizes the complexity of the microcirculatory regulation. The decrease in blood viscosity in extreme hemodilution impairs microvascular flow, since a threshold capillary pressure is necessary to maintain capillary patency and allow for the passage of RBCs (6). In addition, capillary pressure also depends on the gradient between arteriolar and venular pressures (35), which acts as the driving pressure for the microcirculatory flow. Arteriolar vasoconstriction induced by catecholaminergic response (21, 40) can lower capillary pressure because of its effect on the driving pressure and by reductions in capillary hematocrit and viscosity (21). Another factor that might decrease the perfusion pressure and disrupt the microcirculation is the increase in venous pressure (37). Accordingly, we found that mesenteric venous pressure was higher in hemodilution than in hemorrhage and sham groups. Providing that the reduction in arterial viscosity was similar in all vascular beds, differences in vascular tone might explain regional heterogeneities (39).

Alterations in the microcirculation of intestinal mucosa might affect its barrier function with subsequent translocation of bacteria or their products to the bloodstream, a conceivable mechanism of multiorgan failure in critically ill patients (12). As shown in our study, hemodilution induced mucosal ischemia; accordingly, during cardiopulmonary bypass, hemodilution is associated with intestinal mucosal injury (29). Yet the monitoring of the effects of isovolemic hemodilution on tissue perfusion is a complex issue. For example, in healthy volunteers, $\dot{V}_{O_2}$ and lactate remain unchanged during hemodilution to Hb levels of 4.5–5.0 g/dl (30, 43). Gastrointestinal capnography is also unable to show the deleterious effects of hemodilution (15). However, in our experiments an Hb level of 5.0 g/dl induced severe impairment of the intestinal microcirculation. In contrast with experimental and clinical studies showing that sublingual microcirculation fails to reflect the alterations of villi perfusion in septic shock (14, 20), during hemodilution, alterations in sublingual and intestinal microcirculation were parallel. From a clinical standpoint, our study gives experimental basis to support the sublingual window for clinical monitoring of the effects of hemodilution on tissue perfusion.

As supported by the behavior of $\dot{V}_{O_2}$, RER, and lactate (8), a similar degree of anaerobic metabolism developed in hemodilution and hemorrhage. The reductions in systemic and intestinal $\dot{V}_{O_2}$ and the increase in lactic acidosis and in RER were comparable. The rise in RER might identify the anaerobic threshold not only during the increasing $\dot{D}_{O_2}$ that characterizes progressive muscular workload as in exercise (42), but also in the other extreme of the physiological state, during the development of O_2 supply dependency (10, 17). Limitation in the

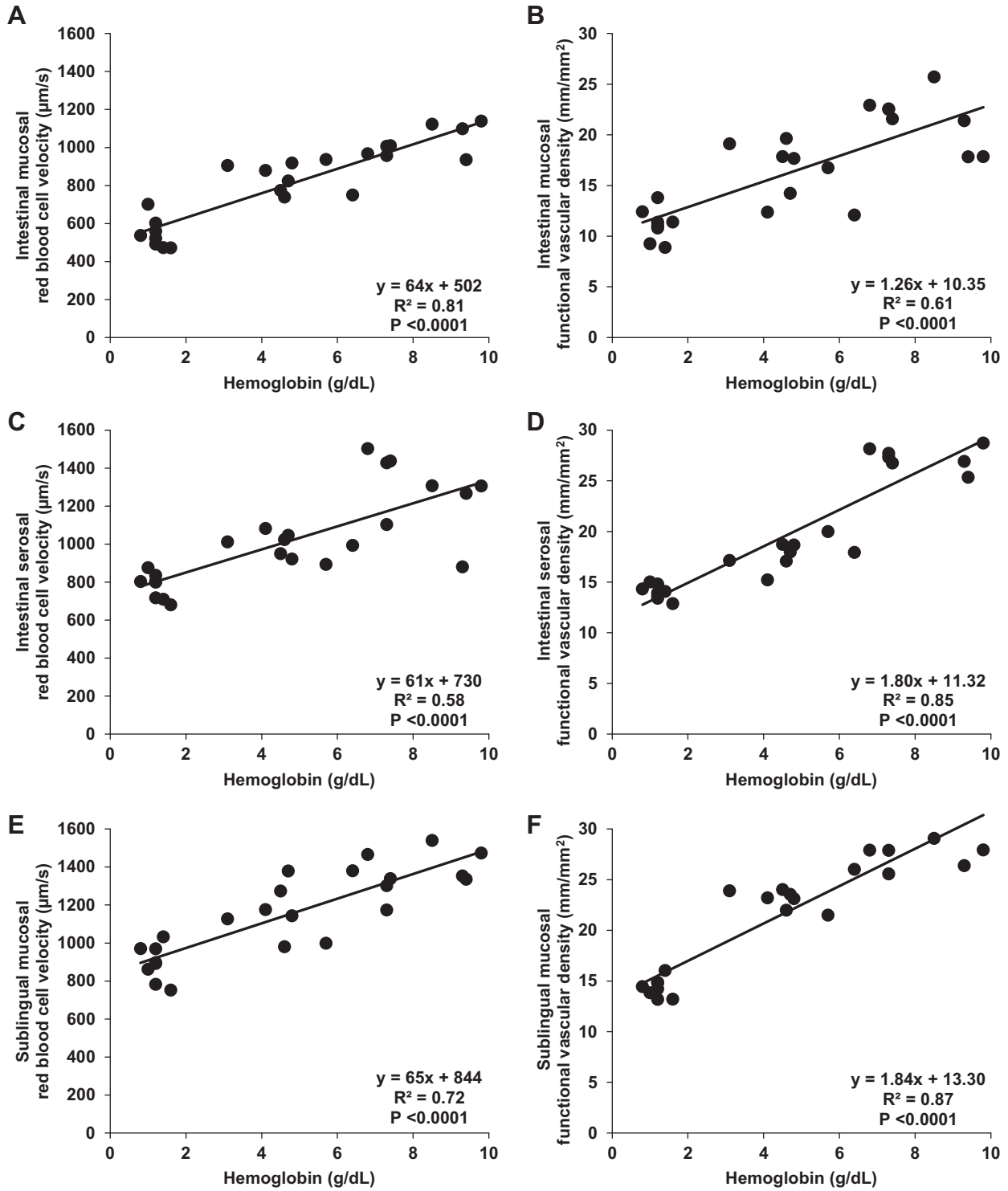

Fig. 5. Correlations between Hb levels and the microcirculatory variables in hemodilution. *A*: intestinal mucosal red blood cell velocity. *B*: intestinal mucosal functional vascular density. *C*: intestinal serosal red blood cell velocity. *D*: intestinal serosal functional vascular density. *E*: sublingual mucosal red blood cell velocity. *F*: sublingual mucosal functional vascular density. There were significant correlations between Hb levels and the microvascular variables in intestinal mucosa and serosa, and in sublingual mucosa.

rate of $\dot{V}O_2$, however, developed at higher $\dot{D}O_2$ and lower fractional O_2 extraction in hemodilution. As previously described, anemic hypoxia is characterized by a defective O_2 extraction in response to falls in $\dot{D}O_2$ (9). Our findings ruled out the short capillary transit time as an explanation for the lower O_2 extraction, at least in the studied territories, since RBC velocity was low. The concurrence of high regional blood flow with severe microvascular hypoperfusion in intestinal serosa and mucosa, along with increased mucosal heterogeneity (41), suggest that microcirculatory shunting might be the underlying mechanism.

The most striking finding of this study was that ΔP_{CO_2} and systemic and intestinal venoarterial CO_2 gradients remained unchanged, despite the severe microcirculatory hypoperfusion. ΔP_{CO_2} has been considered a surrogate of mucosal perfusion (14, 16). Our results, however, suggest that the relationship might be more complex. Venoarterial and tissue-arterial P_{CO_2} gradients result from interactions among aerobic and anaerobic $\dot{V}_{CO_2}$, CO_2 dissociation curve, and tissue perfusion (16). During O_2 supply dependency, opposite changes in aerobic and anaerobic $\dot{V}_{CO_2}$ occur. Aerobic $\dot{V}_{CO_2}$ decreases because of a fall in aerobic metabolism, whereas anaerobic $\dot{V}_{CO_2}$ starts due to bicarbonate buffering of protons derived from fixed acids. Total $\dot{V}_{CO_2}$ does not increase, as shown in our experiments; but as $\dot{V}_{O_2}$ further falls, the RER rises. The relative increment of $\dot{V}_{CO_2}$ with respect to $\dot{V}_{O_2}$ can only cause venous and tissue hypercarbia during tissue hypoperfusion, in which CO_2 removal is reduced. The lack of change in mucosal P_{CO_2} found in hemodilution implies the presence of an effective CO_2 clearance. Therefore, a putative explanation for the absence of intramucosal acidosis might be an increased CO_2 washout from deeper intestinal layers. Since total intestinal blood flow increased but villi and serosal perfusion decreased, we can speculate that given its high solubility, mucosal CO_2 might have been eliminated by means of an increased muscular blood flow.

The main limitation of this study resides in the use of SDF technology for microcirculation assessment. Since the technique is based on Hb absorbance, hemodilution might have altered the RBC visualization. A previous study has validated OPS videomicroscopy during isovolemic hemodilution (26), but at Hb levels higher than those reached in our study (3.8 g/dl). Yet many reasons support the adequacy of our measurements. First, in the validation study (26) there was no underestimation of capillary density by OPS, compared with standard intravital fluorescence microscopy with the increasing levels of hemodilution. The bias was zero within a wide range of Hb, from 14.6 ± 0.7 to 3.8 ± 0.2 g/dl. This suggests that further hemodilution should not modify the difference between OPS and standard videomicroscopy. Second, SDF videomicroscopy is an improved technology, which enhances visualization of the microcirculation. Third, RBC velocity and proportion of perfused vessels cannot be underestimated by SDF videomicroscopy because both rely on the identification of moving RBC. Once a moving RBC is identified by the space-time diagram or by the eye, the measurements are precise and not affected by the hematocrit. Last, in the first step of hemodilution, with a mean Hb of 5.0 g/dl, a value high enough to dissipate any doubts about the technique's performance, severe alterations in densities and velocities were present in every vascular territory. In addition, at this stage a trend of higher compromise in hemodilution than in hemorrhage was observed. This trend reached statistical significance in the intestinal serosa.

Another limitation of this study was that we only considered the intestinal serosa and mucosa, and the sublingual mucosal microcirculation. The microvascular behavior might have been different in other territories.

In summary, the major findings of our study were as follows. First, in extreme isovolemic hemodilution, there is a dissociation between systemic and regional hemodynamics, and microcirculation. Second, although cardiac output and mesenteric blood flow were increased, there was a severe compromise in intestinal and sublingual microcirculation. The microvascular disorders involve the diffusional and convective components of microvascular flow. Hence, these microcirculatory derangements seem to be the underlying mechanism for the defect in O_2 extraction, and not the failure in the discharge of O_2 from Hb. Finally, our results ruled out the hypothesis that the lack of modification in ΔP_{CO_2} results from the preservation of villi perfusion and suggest that CO_2 clearance was achieved in the deeper intestinal layers.

GRANTS

This work was supported by Grant PICT 2010-00495, Agencia Nacional de Promoción Científica y Tecnológica, Argentina.

DISCLOSURES

Dr. Ince has developed SDF imaging and is listed as inventor on related patents commercialized by MicroVision Medical (MVM) under a license from the Academic Medical Center. He has been a consultant for MVM in the past, but has not been involved with this company for more than 5 years now, except that he still holds shares. Braedius Medical, a company owned by a relative of Dr. Ince, has developed and designed a handheld microscope called CytoCam-IDF imaging. Dr. Ince has no financial relation with Braedius Medical of any sort, i.e., he never owned shares or received consultancy or speaker fees from Braedius Medical. All other authors declare that they have no competing interests.

AUTHOR CONTRIBUTIONS

G.F., V.S.K.E., E.M., H.S.C., C.C., G.M., M.O.P., E.E., C.I., and A.D. conception and design of research; G.F., V.S.K.E., E.M., H.S.C., C.C., G.M., M.O.P., and A.D. performed experiments; G.F. and A.D. interpreted results of experiments; G.F., V.S.K.E., E.M., H.S.C., C.C., G.M., M.O.P., E.E., C.I., and A.D. approved final version of manuscript; V.S.K.E., E.E., C.I., and A.D. edited and revised manuscript; A.D. prepared figures; A.D. drafted manuscript.

REFERENCES

1. **Biro GP, Beresford-Kroeger D.** Myocardial blood flow and O_2-supply following dextran-haemodilution and methaemoglobinaemia in the dog. *Cardiovasc Res* 13: 459–468, 1979.
2. **Biro GP.** Comparison of acute cardiovascular effects and oxygen-supply following haemodilution with dextran, stroma-free haemoglobin solution and fluorocarbon suspension. *Cardiovasc Res* 16: 194–204, 1982.
3. **Boerma EC, Mathura KR, van der Voort PH, Spronk PE, Ince C.** Quantifying bedside-derived imaging of microcirculatory abnormalities in septic patients: a prospective validation study. *Crit Care* 9: R601–R606, 2005.
4. **Bourke DL, Smith TC.** Estimating allowable hemodilution. *Anesthesiology* 41: 609–612, 1974.
5. **Cabrales P, Martini J, Intaglietta M, Tsai AG.** Blood viscosity maintains microvascular conditions during normovolemic anemia independent of blood oxygen-carrying capacity. *Am J Physiol Heart Circ Physiol* 291: H581–H590, 2006.
6. **Cabrales P, Tsai AG, Intaglietta M.** Microvascular pressure and functional capillary density in extreme hemodilution with low and high plasma viscosity expanders. *Am J Physiol Heart Circ Physiol* 287: H363–H373, 2004.
7. **Cabrales P, Tsai AG, Frangos JA, Briceño JC, Intaglietta M.** Oxygen delivery and consumption in the microcirculation after extreme hemodilution with perfluorocarbons. *Am J Physiol Heart Circ Physiol* 287: H320–H330, 2004.
8. **Cain SM.** Appearance of excess lactate in anesthetized dogs during anemic and hypoxic hypoxia. *Am J Physiol* 209: 604–610, 1965.
9. **Cain SM.** Oxygen delivery and uptake in dogs during anemic and hypoxic hypoxia. *J Appl Physiol Respir Environ Exerc Physiol* 42: 228–234, 1977.
10. **Cohen IL, Sheikh FM, Perkins RJ, Feustel PJ, Foster ED.** Effect of hemorrhagic shock and reperfusion on the respiratory quotient in swine. *Crit Care Med* 23: 545–552, 1995.
11. **Crystal GJ, Rooney MW, Salem MR.** Myocardial blood flow and oxygen consumption during isovolemic hemodilution alone and in com-

bination with adenosine-induced controlled hypotension. *Anesth Analg* 67: 539–547, 1988.
12. **Deitch EA.** The role of intestinal barrier failure and bacterial translocation in the development of systemic infection and multiple organ failure. *Arch Surg* 125: 403–404, 1990.
13. **Dobbe JG, Streekstra GJ, Atasever B, van Zijderveld R, Ince C.** Measurement of functional microcirculatory geometry and velocity distributions using automated image analysis. *Med Biol Eng Comput* 46: 659–670, 2008.
14. **Dubin A, Edul VS, Pozo MO, Murias G, Canullán CM, Martins EF, Ferrara G, Canales HS, Laporte M, Estenssoro E, Ince C.** Persistent villi hypoperfusion explains intramucosal acidosis in sheep endotoxemia. *Crit Care Med* 36: 535–542, 2008.
15. **Dubin A, Estenssoro E, Murias G, Pozo MO, Sottile JP, Barán M, Piacentini E, Canales HS, Etcheverry G.** Intramucosal-arterial P_{CO_2} gradient does not reflect intestinal dysoxia in anemic hypoxia. *J Trauma* 57: 1211–1217, 2004.
16. **Dubin A, Estenssoro E.** Mechanisms of tissue hypercarbia in sepsis. *Front Biosci* 13: 1340–1351, 2008.
17. **Dubin A, Murias G, Estenssoro E, Canales H, Sottile P, Badie J, Barán M, Rossi S, Laporte M, Pálizas F, Giampieri J, Mediavilla D, Vacca E, Botta D.** End-tidal CO_2 pressure determinants during hemorrhagic shock. *Intensive Care Med* 26: 1619–1623, 2000.
18. **Dubin A, Pozo MO, Ferrara G, Murias G, Martins E, Canullán C, Canales HS, Kanoore Edul VS, Estenssoro E, Ince C.** Systemic and microcirculatory responses to progressive hemorrhage. *Intensive Care Med* 35: 556–564, 2009.
19. **Edul VS, Ferrara G, Pozo MO, Murias G, Martins E, Canullén C, Canales HS, Estenssoro E, Ince C, Dubin A.** Failure of nitroglycerin (glyceryl trinitrate) to improve villi hypoperfusion in endotoxaemic shock in sheep. *Crit Care Resusc* 13: 252–261, 2011.
20. **Edul VS, Ince C, Navarro N, Previgliano L, Risso-Vazquez A, Rubatto PN, Dubin A.** Dissociation between sublingual and gut microcirculation in the response to a fluid challenge in postoperative patients with abdominal sepsis. *Ann Intensive Care* 4: 39, 2014.
21. **Fahraeus R, Lindqvist T.** The viscosity of the blood in narrow capillary tubes. *Am J Physiol* 96: 562–568, 1931.
22. **Fan FC, Chen RY, Schuessler GB, Chien S.** Effects of hematocrit variations on regional hemodynamics and oxygen transport in the dog. *Am J Physiol Heart Circ Physiol* 238: H545–H552, 1980.
23. **Goedhart PT, Khalilzada M, Bezemer R, Merza J, Ince C.** Sidestream dark field (SDF) imaging: a novel stroboscopic LED ring-based imaging modality for clinical assessment of the microcirculation. *Opt Express* 15: 15101–15104, 2007.
24. **Gutierrez G, Marini C, Acero AL, Lund N.** Skeletal muscle P_{O_2} during hypoxemia and isovolemic anemia. *J Appl Physiol (1985)* 68: 2047–2053, 1990.
25. **Gutierrez G.** The rate of oxygen release and its effect on capillary O_2 tension: a mathematical analysis. *Respir Physiol* 63: 79–96, 1986.
26. **Harris AG, Sinitsina I, Messmer K.** Validation of OPS imaging for microvascular measurements during isovolumic hemodilution and low hematocrits. *Am J Physiol Heart Circ Physiol* 282: H1502–H1509, 2002.
27. **Hudetz AG, Wood JD, Biswal BB, Krolo I, Kampine JP.** Effect of hemodilution on RBC velocity, supply rate, and hematocrit in the cerebral capillary network. *J Appl Physiol (1985)* 87: 505–509, 1999.
28. **Hudetz AG, Wood JD, Kampine JP.** 7-Nitroindazole impedes erythrocyte flow response to isovolemic hemodilution in the cerebral capillary circulation. *J Cereb Blood Flow Metab* 20: 220–224, 2000.
29. **Huybregts RA, de Vroege R, Jansen EK, van Schijndel AW, Christiaans HM, van Oeveren W.** The association of hemodilution and transfusion of red blood cells with biochemical markers of splanchnic and renal injury during cardiopulmonary bypass. *Anesth Analg* 109: 331–339, 2009.
30. **Lieberman JA, Weiskopf RB, Kelley SD, Feiner J, Noorani M, Leung J, Toy P, Viele M.** Critical oxygen delivery in conscious humans is less than 7.3 ml $O_2 \times kg^{-1} \times min^{-1}$. *Anesthesiology* 92: 407–413, 2000.
31. **Lindbom L, Mirhashemi S, Intaglietta M, Arfors KE.** Increase in capillary blood flow and relative haematocrit in rabbit skeletal muscle following acute normovolaemic anaemia. *Acta Physiol Scand* 134: 503–512, 1988.
32. **Pozo MO, Kanoore Edul VS, Ince C, Dubin A.** Comparison of different methods for the calculation of the microvascular flow index. *Crit Care Res Pract* 2012: 102483, 2012.
33. **Sakai H, Sato T, Maekawa Y, Tsuchida E.** Capillary blood flow during severe hemodilution observed by a noninvasive transcutaneous technique using flash epi-illumination. *Microvasc Res* 64: 120–126, 2002.
34. **Schumacker PT, Cain SM.** The concept of a critical oxygen delivery. *Intensive Care Med* 13: 223–229, 1987.
35. **Schwarte LA, Fournell A, van Bommel J, Ince C.** Redistribution of intestinal microcirculatory oxygenation during acute hemodilution in pigs. *J Appl Physiol (1985)* 98: 1070–1075, 2005.
36. **Sinaasappel M, van Iterson M, Ince C.** Microvascular oxygen pressure in the pig intestine during haemorrhagic shock and resuscitation. *J Physiol* 514: 245–53, 1999.
37. **Taylor AE, Moore TM.** Capillary fluid exchange. *Adv Physiol Ed* 277: S203–S210, 1999.
38. **Tsai AG, Vandegriff KD, Intaglietta M, Winslow RM.** Targeted O_2 delivery by low-P50 hemoglobin: a new basis for O_2 therapeutics. *Am J Physiol Heart Circ Physiol* 285: H1411–H1419, 2003.
39. **Tsui AK, Marsden PA, Mazer CD, Sled JG, Lee KM, Henkelman RM, Cahill LS, Zhou YQ, Chan N, Liu E, Hare GM.** Differential HIF and NOS responses to acute anemia: defining organ-specific hemoglobin thresholds for tissue hypoxia. *Am J Physiol Regul Integr Comp Physiol* 307: R13–R25, 2014.
40. **Van Woerkens EC, Trouwborst A, Duncker DJ, Koning MM, Boomsma F, Verdouw PD.** Catecholamines and regional hemodynamics during isovolemic hemodilution in anesthetized pigs. *J Appl Physiol (1985)* 72: 760–769, 1992.
41. **Walley KR.** Heterogeneity of oxygen delivery impairs oxygen extraction by peripheral tissues: theory. *J Appl Physiol* 81: 885–894, 1996.
42. **Wasserman K, Whipp BJ, Koyl SN, Beaver WL.** Anaerobic threshold and respiratory gas exchange during exercise. *J Appl Physiol* 35: 236–243, 1973.
43. **Weiskopf RB, Viele MK, Feiner J, Kelley S, Lieberman J, Noorani M, Leung JM, Fisher DM, Murray WR, Toy P, Moore MA.** Human cardiovascular and metabolic response to acute, severe isovolemic anemia. *JAMA* 279: 217–221, 1998.